Hydrological Cycles over the Congo and Upper Blue Nile Basins: Evaluation of General Circulation Model Simulations and Reanalysis Products

Mohamed S. Siam

Ralph M. Parsons Laboratory, Massachusetts Institute of Technology, Cambridge, Massachusetts

Marie-Estelle Demory

National Centre for Atmospheric Science, Department of Meteorology, University of Reading, Reading, United Kingdom

Elfatih A. B. Eltahir

Ralph M. Parsons Laboratory, Massachusetts Institute of Technology, Cambridge, Massachusetts

ABSTRACT

The simulations and predictions of the hydrological cycle by general circulation models (GCMs) are characterized by a significant degree of uncertainty. This uncertainty is reflected in the range of Intergovernmental Panel on Climate Change (IPCC) GCM predictions of future changes in the hydrological cycle, particularly over major African basins. The confidence in GCM predictions can be increased by evaluating different GCMs, identifying those models that succeed in simulating the hydrological cycle under current climate conditions, and using them for climate change studies. Reanalyses are often used to validate GCMs, but they also suffer from an inaccurate representation of the hydrological cycle. In this study, the aim is to identify GCMs and reanalyses' products that provide a realistic representation of the hydrological cycle over the Congo and upper Blue Nile (UBN) basins. Atmospheric and soil water balance constraints are employed to evaluate the models' ability to reproduce the observed streamflow, which is the most accurate measurement of the hydrological cycle. Among the ECMWF Interim Re-Analysis (ERA-Interim), NCEP–NCAR reanalysis, and 40-yr ECWMF Re-Analysis (ERA-40), ERA-Interim shows the best performance over these basins: it balances the water budgets and accurately represents the seasonal cycle of the hydrological variables. The authors find that most GCMs used by the IPCC overestimate the hydrological cycle compared to observations. They observe some improvement in the simulated hydrological cycle with increased horizontal resolution, which suggests that some of the high-resolution GCMs are better suited for climate change studies over Africa.

1. Introduction

General circulation models (GCMs) are the best available tools to predict climate change associated with future scenarios of greenhouse gas concentrations. However, an analysis of their outputs reveals that these models do not accurately reproduce the past and current climates. This is particularly the case for hydrological variables (e.g., precipitation) that show large inconsistency, especially over Africa (Christensen et al. 2007). Over large basins, such as African basins, model outputs are often statistically or dynamically downscaled for impact studies on water resources, floods and droughts, and agriculture. However, many uncertainties lie behind the choice of a downscaling method, which may amplify inherent errors in GCM outputs and increase uncertainties associated with climate change predictions of the hydrological cycle at smaller scale, such as over river basins (Boé et al. 2009). These errors are reflected in the disagreement between GCM predictions on the sign and magnitude of changes in river runoff over major African basins (Strzepek and Yates 1996; Conway and Hulme 1996; Yates and Strzepek 1998; Nohara et al. 2006; Kim et al. 2008). Furthermore, reanalysis products such as the European Centre for Medium-Range Weather Forecasts (ECMWF) Interim Re-Analysis

Corresponding author address: Mohamed Siam, Ralph M. Parsons Laboratory, Massachusetts Institute of Technology, 15 Vassar St., Cambridge, MA 02139.
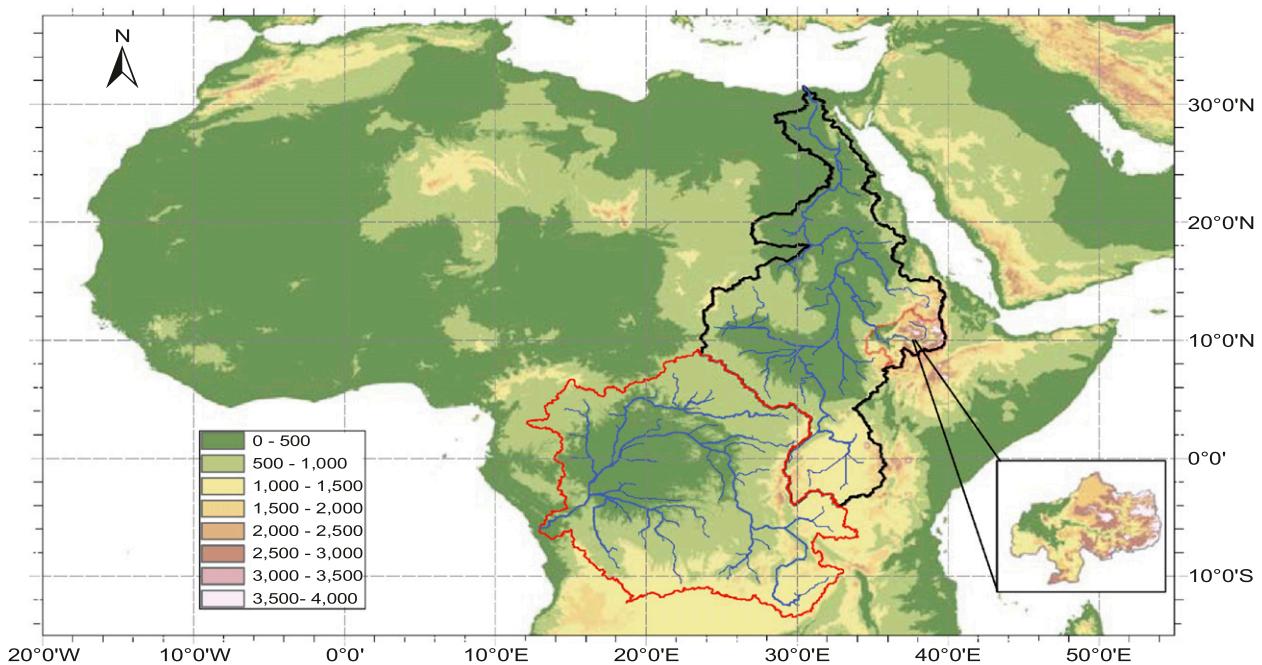E-mail: msiam@mit.edu

FIG. 1. Topographic map of Northern Africa and the Middle East (m) overlaid by the Nile (black), Congo (red), and UBN basins (orange).

(ERA-Interim; Dee et al. 2011; Berrisford et al. 2011) and the National Centers for Environmental Prediction– National Center for Atmospheric Research reanalysis (NCEP–NCAR; Kalnay et al. 1996) are often used to validate GCMs or to drive regional climate models (RCMs), so that a use of biased reanalysis products may lead to errors in assessing model performances. The choice of reanalyses and GCMs is therefore crucial and can have large consequences on the decision-making process related to climate change. We believe that we can guide our choice of GCMs and reanalyses by evaluating them over major African basins and by only choosing the models that can accurately reproduce the observed hydrological cycle. Such evaluation may increase our confidence in GCM predictions of changes in the hydrological cycle over African basins associated with climate change.

Several methods are used to evaluate the performance of climate models in simulating climate features at different spatial scales (Schaller et al. 2011). The methods depend on the variables or phenomena that are evaluated. The most common evaluation methods can be grouped into three categories (Raisanen 2007; Randall et al. 2007): 1) statistical measures or "performance metrics" (e.g., mean errors, correlations, root-mean-square errors, and performance indices) that compare model outputs with observations and provide information on the performance of the model without detailing the cause of biases (e.g., Gleckler et al. 2008; Perkins et al. 2007); 2) diagnostics that provide

information on the sources of model discrepancies and include a detailed analysis to identify processes connected to the errors (e.g., analysis of energy and water cycles, and analysis of atmospheric and land processes); and 3) the evaluation of climate models based on the representation of specific events (e.g., monsoons and ENSO teleconnections). These approaches are widely used to validate climate models and reanalysis products (Dee et al. 2011; Johns et al. 2006; Uppala et al. 2005; Kalnay et al. 1996).

In this study, we consider the second approach to assess GCMs and reanalyses performance in representing the hydrological cycle over two major African basins: the upper Blue Nile (UBN) basin and the Congo basin, over which GCM predictions are highly uncertain (Christensen et al. 2007). We use the atmospheric and soil water balance constraints to evaluate GCMs and reanalyses. Those constraints state that the long-term average of river flow should approximately balance precipitation minus evaporation [Eq. (3)] and should equal atmospheric moisture convergence [Eq. (7)]. This

TABLE 1. Summary of the UBN and Congo basins characteristics.

	Congo	UBN
Area (km^2)	3.8×10^6	175×10^3
Mean annual precipitation (mm day^{-1})	1553	1224
Mean annual streamflow (km^3)	1270	46

TABLE 2. Summary of reanalysis products and observations data used.

Data	Variables	Coverage period	Horizontal resolution	No. of atmospheric layers
ERA-Interim	Zonal wind (U), meridional wind (V), specific humidity (q) Runoff (R), precipitation (P), evaporation (ET), soil moisture (SM)	1989–2010	$1.5° \times 1.5°$	37 pressure levels (1000–1 mb)
ERA-40	U, V, q, R, P, ET, SM	1979–2002	$2.5° \times 2.5°$	23 pressure levels (1000–1 mb)
NCEP–NCAR	U, V, q, R, P, ET, SM	1979–2002	$2.5° \times 2.5°$	8 pressure levels (1000–300 mb)
NTSG	ET	1983–2006	$0.5° \times 0.5°$	—
CRU TS 3.1	P	1901–2009	$0.5° \times 0.5°$	—

method allows an evaluation based on the ability of GCMs and reanalyses to accurately represent the observed streamflow of the UBN and Congo basins. These approaches are commonly used to estimate components of the hydrological cycle (e.g., evaporation, soil moisture, and atmospheric moisture convergence) that are not or insufficiently available from observations (Karam and Bras 2008a; Seneviratne et al. 2004; Yeh et al. 1998; Oki et al. 1995; Calanca and Ohmura 1994; Rasmusson 1967, 1968). This method also has the advantage to emphasize the ability of GCMs to simulate processes that control the hydrological cycle, which provides a good indicator of the general performance of the model. The hydrological cycle depends on several variables, such as wind, specific humidity, precipitation, soil water storage, evaporation, radiation, and clouds. An inaccurate representation of any of these variables would therefore be reflected in the simulation of precipitation, evaporation, and runoff, which highlights the necessity to thoroughly validate each component of the hydrological cycle and understand how they are connected. A detailed analysis of the different components of hydrological cycle is also important, as GCMs or reanalyses can accurately represent one variable of the hydrological cycle but show large errors in other variables (Trenberth et al. 2007)

By evaluating GCMs and reanalysis products over the Congo and UBN basins using the atmospheric and soil water balance approaches, we aim to (i) investigate their ability in representing the hydrological cycle under present-day climate conditions and (ii) identify the best GCM candidates for climate change studies on water resources over these basins.

2. Study areas

The evaluation of the hydrological cycle in reanalyses and GCMs is applied over two African basins, the upper Blue Nile and Congo basins, which have very different characteristics in size and complexity. The upper Blue

Nile basin is small but highly important as it contributes to approximately 60% of the total Nile streamflow and is spatially very variable because of its high and narrow orography. The Congo basin, on the other hand, is one of the largest basins in Africa (it is approximately 20 times larger than the UBN basin) and has a smoother topography. Evaluating GCMs and reanalyses over these two very different basins allows an evaluation not only of the components of the hydrological cycle but also on the processes associated with the hydrological cycle over each basin.

a. The upper Blue Nile basin

The upper Blue Nile basin is the main source of water for the Nile River. It contributes to approximately 60% of the main flow of the Nile (based on analyses of the period 1945–84, Conway and Hulme 1993). It extends from 7° to 12°5′ N and from 34°5′ to 40°E. The eastern part of the basin has the highest elevation reaching 4000 m above mean sea level and decreasing gradually toward the western outlet of the basin where the elevation is approximately 500 m above mean sea level (Fig. 1). The mean annual rainfall and streamflow of the basin, by Conway and Hulme (1993) and Elshamy et al. (2009), respectively, are shown in Table 1.

b. The Congo basin

The Congo basin is located in the middle of the African continent and extends from 11°S to 9′N and from 14° to 34°E (Fig. 1). The eastern and southern boundaries of the basins are mountainous and the western boundary is the Atlantic Ocean. The variation in topography is small compared to the UBN basin: most of the Congo basin has an elevation below 500 m above mean sea level and higher elevations are only seen close to the east and south of the basin (Fig. 1). The mean annual rainfall and streamflow of the basin, estimated by Samba and Nganga (2011) and Amarasekera et al. (1997), respectively, are shown in Table 1. The seasonal cycle of rainfall has two peaks extending each for 3 months around April

TABLE 3. Summary of GCMs used in this study.

Project	Model	Model expansion	Output resolution	Agency
CMIP3	1) HadGEM1	Hadley Centre Global Environmental Model, version 1	1.875° × 1.25°	Hadley Center for Climate Prediction and Research, Met Office, United Kingdom
	2) MPI ECHAM5	Max Planck Institute ECHAM5	1.875° × 1.87°	Max Planck Institute for Meteorology, Germany
	3) CSIRO MK3.5	Commonwealth Scientific and Industrial Research Organisation Mark, version 3.5	1.875° × 1.86°	CSIRO Atmospheric Research, Australia
	4) CSIRO MK3.0	Commonwealth Scientific and Industrial Research Organisation Mark, version 3.0	1.875° × 1.86°	CSIRO Atmospheric Research, Australia
	5) GFDL CM2.0	Geophysical Fluid Dynamics Laboratory Climate Model, version 2.0	2.5° × 2°	Geophysical Fluid Dynamics Laboratory, United States
	6) BCCR-CM2.0	Bjerknes Centre for Climate Research Bergen Climate Model, version 2.0	2.8° × 2.8°	Bjerknes Center for Climate Research, Norway
	7) MRI-CGCM2.3.2	Meteorological Research Institute Coupled Atmosphere–Ocean General Circulation Model, version 2.3.2	2.8° × 2.8°	Meteorological Research Institute, Japan
	8) NCAR PCM1	NCAR Parallel Climate Model	2.8° × 2.8°	NCAR, National Science Foundation (NSF), U.S. Department of Energy (DOE), National Aeronautics and Space Administration (NASA), and National Oceanic and Atmospheric Administration (NOAA), United States
	9) CNRM-CM3	Centre National de Recherches Météorologiques Coupled Global Climate Model, version 3	2.8° × 2.8°	National Center of Meteorological Research, France
	10) IAP FGOALS	Institute of Atmospheric Physics Flexible Global Ocean–Atmosphere–Land System Model	2.8° × 2.8°	Institute of Atmospheric Physics, Chinese Academy of Sciences, China
	11) CCCma CGCM3.1(T63)	Canadian Centre for Climate Modelling and Analysis Coupled GCM 3.1 (T63 resolution)	2.8° × 2.7°	Canadian Centre for Climate Modelling and Analysis, Canada
	12) HadCM3	Third climate configuration of the Met Office Unified Model	3.75° × 2.5°	Hadley Center for Climate Prediction and Research, Met Office, United Kingdom
	13) IPSL-CM4	L'Institut Pierre-Simon Laplace Coupled Model version 4	3.75° × 2.5°	L'Institut Pierre-Simon Laplace, France
	14) MIUB-ECHO-G	Meteorological Institute of the University of Bonn, ECHO-G Model	3.75° × 2.7°	Meteorological Institute of the University of Bonn, Germany
	15) CCCma CGCM3.1(T47)	Canadian Centre for Climate Modelling and Analysis Coupled GCM 3.1 (T47 resolution)	3.75° × 3.7°	Canadian Centre for Climate Modelling and Analysis, Canada
	16) GISS-AOM3.1	Goddard Institute for Space Studies, Atmosphere–Ocean Model 3.1	4° × 3°	Goddard Institute for Space Studies, United States
	17) INM-CM3.0	Institute of Numerical Mathematics Coupled Model, version 3.0	5° × 4°	Institute of Numerical Mathematics, Russia
CMIP5	1) MRI-CGCM3	Meteorological Research Institute Coupled Atmosphere–Ocean General Circulation Model, version 3	1.12° × 1.12°	Meteorological Research Institute, Japan
	2) CNRM-CM5	Centre National de Recherches Météorologiques Coupled Global Climate Model, version 5	1.4° × 1.4°	National Center of Meteorological Research, France
	3) INM-CM4.0	Institute of Numerical Mathematics Coupled Model, version 4.0	2° × 1.5°	Institute of Numerical Mathematics, Russia

TABLE 3. (Continued)

Project	Model	Model expansion	Output resolution	Agency
	4) HadGEM2-CC	Hadley Centre Global Environmental Model, version 2 (Carbon Cycle)	1.875° × 1.25°	Hadley Center for Climate Prediction and Research, Met Office, United Kingdom
	5) CSIRO	Commonwealth Scientific and Industrial Research Organisation	1.85° × 1.85°	CSIRO Atmospheric Research, Australia
	6) IPSL-CM5-MR	L'Institut Pierre-Simon Laplace Coupled Model, version 5, coupled with NEMO, mid resolution	2.5° × 1.26°	Institute Pierre Simon Laplace, France
	7) NorESM1-M	Norwegian Earth System Model, version 1 (medium resolution)	2.5° × 1.9°	Norwegian Climate Centre, Norway
	8) GISS-E2H	Goddard Institute for Space Studies Model E, coupled with the HYCOM ocean model	2.5° × 2°	Goddard Institute for Space Studies, United States
	9) GFDL CM3	Geophysical Fluid Dynamics Laboratory Climate Model, version 3	2.5° × 2°	Geophysical Fluid Dynamics Laboratory, United States
	10) BCC-CSM1	Beijing Climate Center, Climate System Model, version 1	2.8° × 2.8°	Beijing Climate Center, China
	11) CanESM2	Second Generation Canadian Earth System Model	2.8° × 2.8°	Canadian Centre for Climate Modelling and Analysis, Canada

and October and each accounting for approximately 32% of the total annual rainfall (Samba and Nganga 2011). The annual average discharge is usually constant with two peaks in May and December (Amarasekera et al. 1997).

3. Methodology and datasets

a. Methodology

The atmospheric and soil water balance approaches are applied for the Congo and the UBN basins, which have different climatic conditions, spatial scales, and complexity of topography. The water balance is checked for soil and the atmosphere, as the long-term averages of the net atmospheric moisture fluxes and the excess of rainfall over evaporation must be in balance with each other and with the observed streamflow. The moisture fluxes and the convergence of atmospheric moisture are calculated using the winds and specific humidity fields from the atmospheric data.

The formulations of the atmospheric and soil water balance equations used in this study are similar to that of Peixoto and Oort (1992). The soil water balance equation may be written as

$$S = P - E - R_0 - R_u, \tag{1}$$

where S is the rate of change in soil water storage, P is the precipitation rate, E is the evaporation rate, R_0 is the surface runoff, and R_u is the subsurface runoff. When this equation is spatially averaged over a specified basin and taking the long-term average of all its components, it takes the form

$$\{\overline{S}\} = \{\overline{P}\} - \{\overline{E}\} - \{\overline{R_0}\} - \{\overline{R_u}\}, \tag{2}$$

where the overbar indicates the temporal average and variables in braces indicate the spatial average over a large basin. Over a long period, the change in storage is found to be two to three orders of magnitude smaller than the other hydrological variables. It can therefore be neglected, which leads to the following equation:

$$\{\overline{P}\} - \{\overline{E}\} = \{\overline{R}\}, \tag{3}$$

where R is the combination of the surface and subsurface runoff rates.

Over shorter time scales, such as a month, the change in water storage cannot be neglected and the streamflow can be estimated using the equation

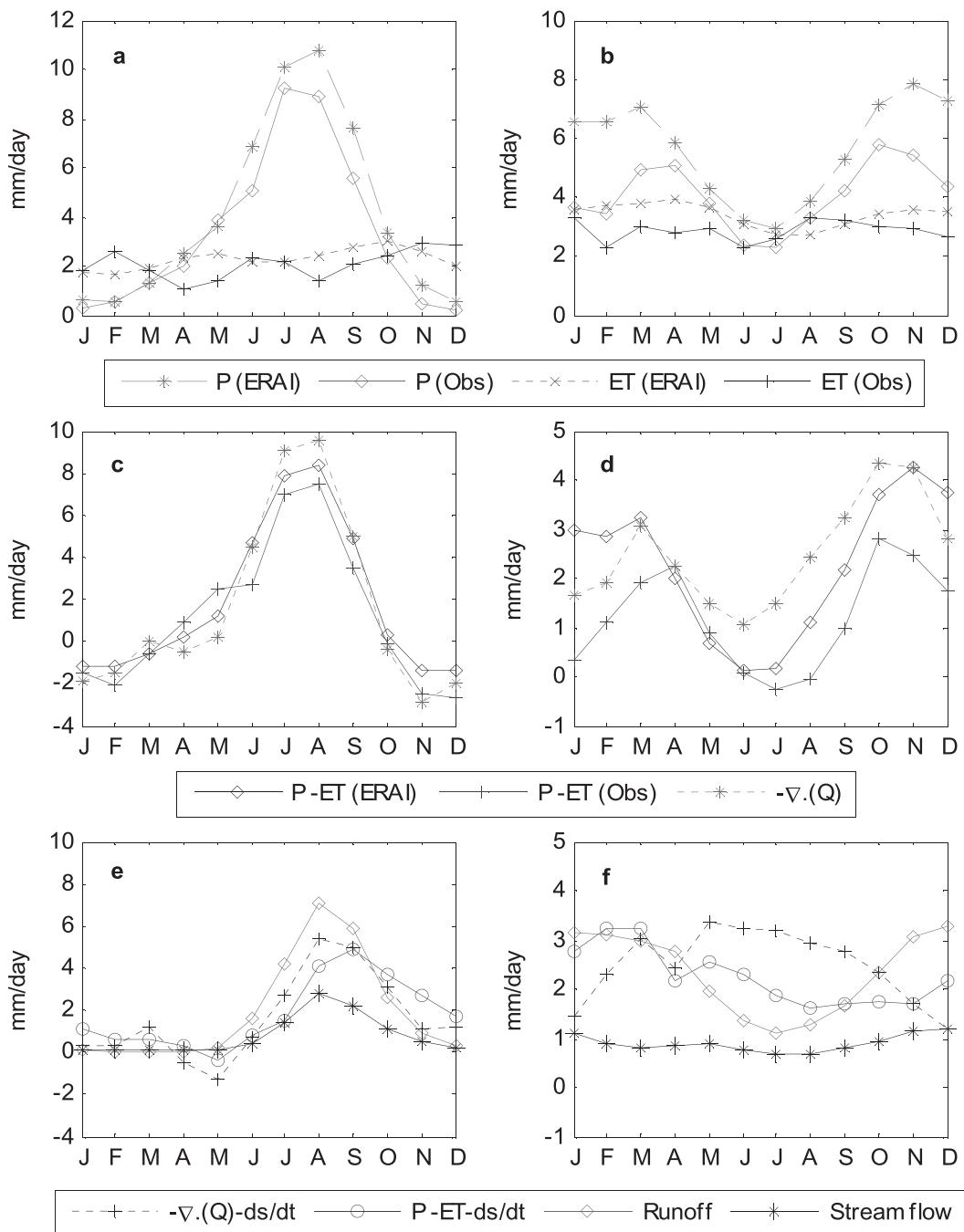$$\{R\} = \{P\} - \{E\} - \{S\}. \tag{4}$$

FIG. 2. Monthly 22-yr (1989–2010) averages values for from (left) the UBN and (right) the Congo basins using: (a),(b) the ERA-Interim data for the precipitation and evaporation with the precipitation of the CRU TS 3.1 data and the evaporation data (NTSG) as observed values; (c),(d) convergence of moisture and difference between precipitation and evaporation of ERA-Interim and CRU precipitation and NTSG evaporation; and (e),(f) observed streamflow, runoff, and estimated runoff from the atmospheric and soil water balance approaches.

The atmospheric water balance is satisfied when the excess of rainfall minus evaporation is in balance with the column integrated atmospheric moisture fluxes. The moisture fluxes $Q(u)$ and $Q(v)$ are calculated by vertically integrating the product of specific humidity q and wind components in the zonal u and meridional v directions from the surface to the top of the atmosphere as follows:

TABLE 4. Summary of results using the reanalysis products over the Congo and upper Blue Nile basins. All values are in millimeters per day.

Basin	Data	P	ET	$P-$ ET	Runoff	$-\mathbf{\nabla}\cdot Q$	ds/dt
Congo basin	ERA-Interim	5.65	3.5	2.15	2.33	2.51	0.001
	ERA-40	1.45	0.76	0.69	0.7	2.3	−0.009
	NCEP–NCAR	5.14	4.25	0.89	1.08	−0.27	0.002
	Obs	4.06	2.83	1.23	0.9	—	—
Upper Blue Nile basin	ERA-Interim	4.09	2.27	1.82	1.93	1.61	0.004
	ERA-40	1.56	0.55	1.06	0.82	1.76	−0.003
	NCEP–NCAR	5.1	2.95	2.15	1.36	1.61	−0.012
	Obs	3.3	2.08	1.22	0.72	—	—

$$Q(v) = \int_0^{P_0} qv\frac{dp}{g}, \quad Q(u) = \int_0^{P_0} qu\frac{dp}{g}, \quad \text{and}$$

$$W(\lambda,\phi,t) = \int_0^{P_0} q\frac{dp}{g}, \tag{5}$$

where W is the mass of water vapor contained in an air column per unit area, W_c is the mass of condensed water in an air column of unit area, and P_0 is the surface pressure.

The atmospheric water balance equation can be written as

$$\frac{\partial W}{\partial t} + \mathbf{\nabla}\cdot Q + \frac{\partial W_c}{\partial t} + \mathbf{\nabla}\cdot Q_c = E - P. \tag{6}$$

This equation can be represented as a control volume where the divergence terms $(\mathbf{\nabla}\cdot Q)$ and $(\mathbf{\nabla}\cdot Q_c)$ account for the exchange of moisture across the boundaries of the control volume and the terms $\partial W/dt$ and $\partial W_c/dt$ are the changes in atmospheric water storage inside the control volume (the subscript c indicates the condensed mass of water vapor).

The amount of condensed water was compared to the total amount of water vapor in an air column and it was found that at least two to three orders of magnitude separate the water vapor content and the condensed water content in form of liquid or ice. The change in storage of water vapor term is usually small compared to the other terms in Eq. (4) when considering relatively long time interval (e.g., monthly or longer) (Yeh et al. 1998; Seneviratne et al. 2004); thus, after taking the temporal and spatial averages, Eq. (6) simplifies to

$$\{\overline{\mathbf{\nabla}\cdot Q}\} = \{\overline{P}\} - \{\overline{E}\} \tag{7}$$

and, using Eq. (4) with Eq. (6) and rearranging, we can write

$$\{\overline{R}\} = -\{\overline{\mathbf{\nabla}\cdot Q}\} - \{\overline{S}\}, \tag{8}$$

where the divergence term is calculated using a central finite difference scheme.

b. Datasets

The methodology detailed above makes use of rain and flow gauge observations and can be systematically applied to several GCM outputs as well as reanalysis products. The precipitation observations are based on the Climatic Research Unit (CRU) TS 3.1 data product, which is the successor of the CRU TS 2.1 (Mitchell and Jones 2005). The evaporation observations are based on the Numerical Terradynamic Simulation Group (NTSG) of the University of Montana global evaporation dataset (Zhang et al. 2010). The stream flows at the outlet of the Congo and UBN basins were available from the Global River Discharge Database (RivDIS v1.1) (Vörösmarty et al. 1998) and personal communications, respectively.

The ERA-Interim product (Dee et al. 2011) is used in this study. The atmospheric variables, which include the zonal and meridional wind components and specific humidity at 37 pressure levels starting from the surface to the top of the stratosphere at 1 mb and at 6-hourly time steps, are used to calculate the atmospheric moisture convergence. Precipitation, evaporation, runoff, and soil moisture over four layers are based on the 12-hourly accumulated fields (Table 2). In addition, the 40-yr ECMWF Re-Analysis (ERA-40) product (Uppala et al. 2005) and the NCEP–NCAR reanalysis product (Kalnay et al. 1996) are also analyzed in this study.

We make use of simulation outputs from 17 GCMs of phase 3 of the World Climate Research Programme (WCRP) Coupled Model Intercomparison Project (CMIP3) multimodel dataset (Meehl et al. 2007), as well as 11 GCMs of the CMIP5 multimodel dataset (Taylor et al. 2012). Monthly average values of precipitation, evaporation, and runoff are used in this analysis (Table 3).

4. Results and discussion

a. The hydrological cycle in reanalysis products

The hydrological cycle of reanalysis products is analyzed in this section for two reasons: (i) reanalysis fields

have the advantage of including assimilated observations and potentially represent the hydrological cycle more realistically than GCMs and; (ii) the same fields provide the lateral boundary conditions for RCM simulations; hence, biases in these products can misleading interpretations of RCM results, so that it is important to choose carefully the reanalysis products used to drive RCMs. In this section, the analysis investigates the representation of the hydrological cycle in ERA-Interim, ERA-40, and NCEP–NCAR over the UBN and Congo basins.

The area of the UBN basin is approximately $2 \times 10^5 \, km^2$, which is close to the smallest area ($1 \times 10^5 \, km^2$) necessary for applying the atmospheric water balance approach to obtain reasonable and accurate results, as discussed by Rasmusson (1971) and Yeh et al. (1998). This can be a problem when analyzing models and reanalyses that have very low resolutions. However, with the availability of higher-resolution climate models and reanalysis data, the atmospheric water balance approach can be applied for smaller areas. The scarcity of upper air observations and complexity of topography add additional factors that might impose difficulties for applying this approach over this region.

The seasonal cycle of precipitation over the UBN basin is closer to observations compared to that of the Congo basin as shown in Figs. 2a,b. However the long-term averages are overestimated for both locations as shown in Table 4. In Figs. 2c,d, the atmospheric water balance is tested. It is shown that the seasonal cycle of atmospheric moisture convergence and precipitation minus evaporation in ERA-Interim agree with that of the observed difference between CRU precipitation and NTSG evaporation over the UBN basin. However, there is an overestimation of moisture convergence from May to August over the Congo basin. This bias is due to the strong convergence of moisture along the western boundary of the basin as shown in Fig. 3a. The difference between the long-term averages of ERA-Interim moisture fluxes and the net precipitation is approximately $0.2 \, mm \, day^{-1}$ over the UBN and Congo basins (Table 4). This small imbalance can be related to the errors that arise from the finite difference scheme used in the calculations or the fact that the precipitation and evaporation values are based on 12-hourly accumulated fields of the forecast model, while the fluxes fields are based on reanalysis of observations (Dee et al. 2011; Berrisford et al. 2011).

To validate the soil water balance, the different estimates of runoff are compared in Figs. 2e,f. The calculated runoff from ERA-Interim model is compared to estimates from Eqs. (4) and (8). The overestimation in precipitation values without a similar overestimation
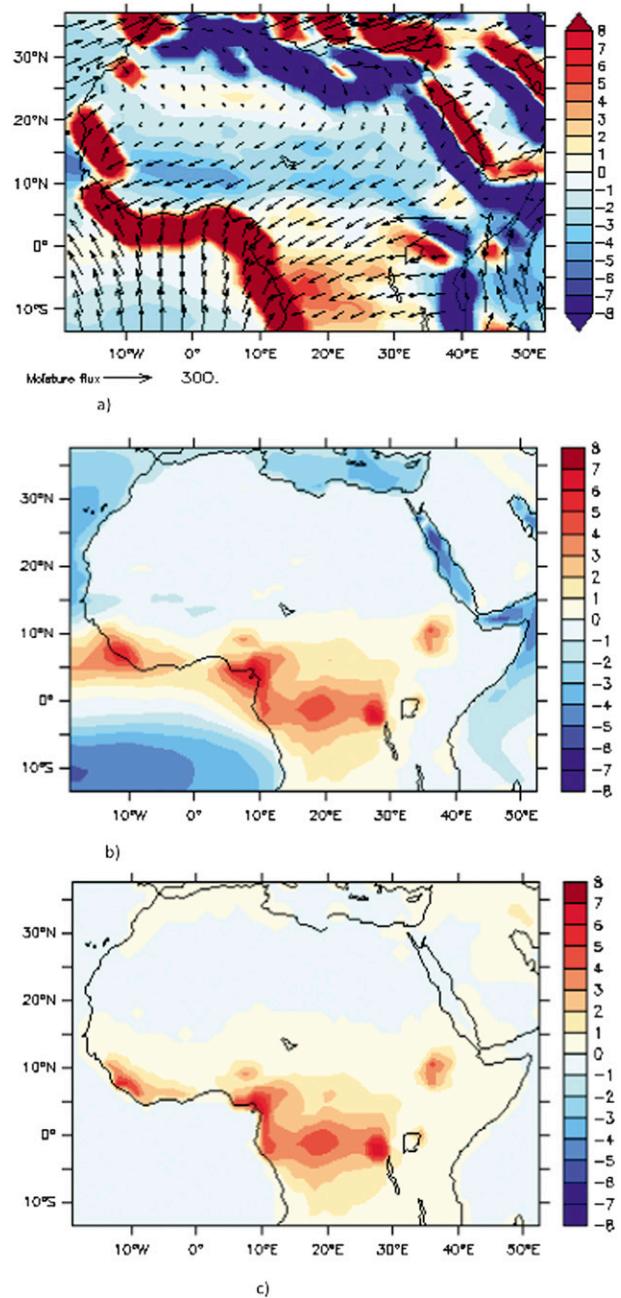

FIG. 3. Spatial distribution using the ERA-Interim data of the 22-yr (1989–2010) average of (a) convergence of atmospheric moisture ($mm \, day^{-1}$) overlaid by the moisture fluxes field ($kg \, m^{-1} \, s^{-1}$), (b) difference between precipitation and evaporation ($mm \, day^{-1}$), and (c) runoff ($mm \, day^{-1}$).

in evaporation enhanced the estimates of runoff, which is approximately equal to more than double the observed stream flows for both regions as shown in Table 4. This significant overestimation was probably higher than the soil storage capacity to hold and redistribute water over the year and to generate runoff that has
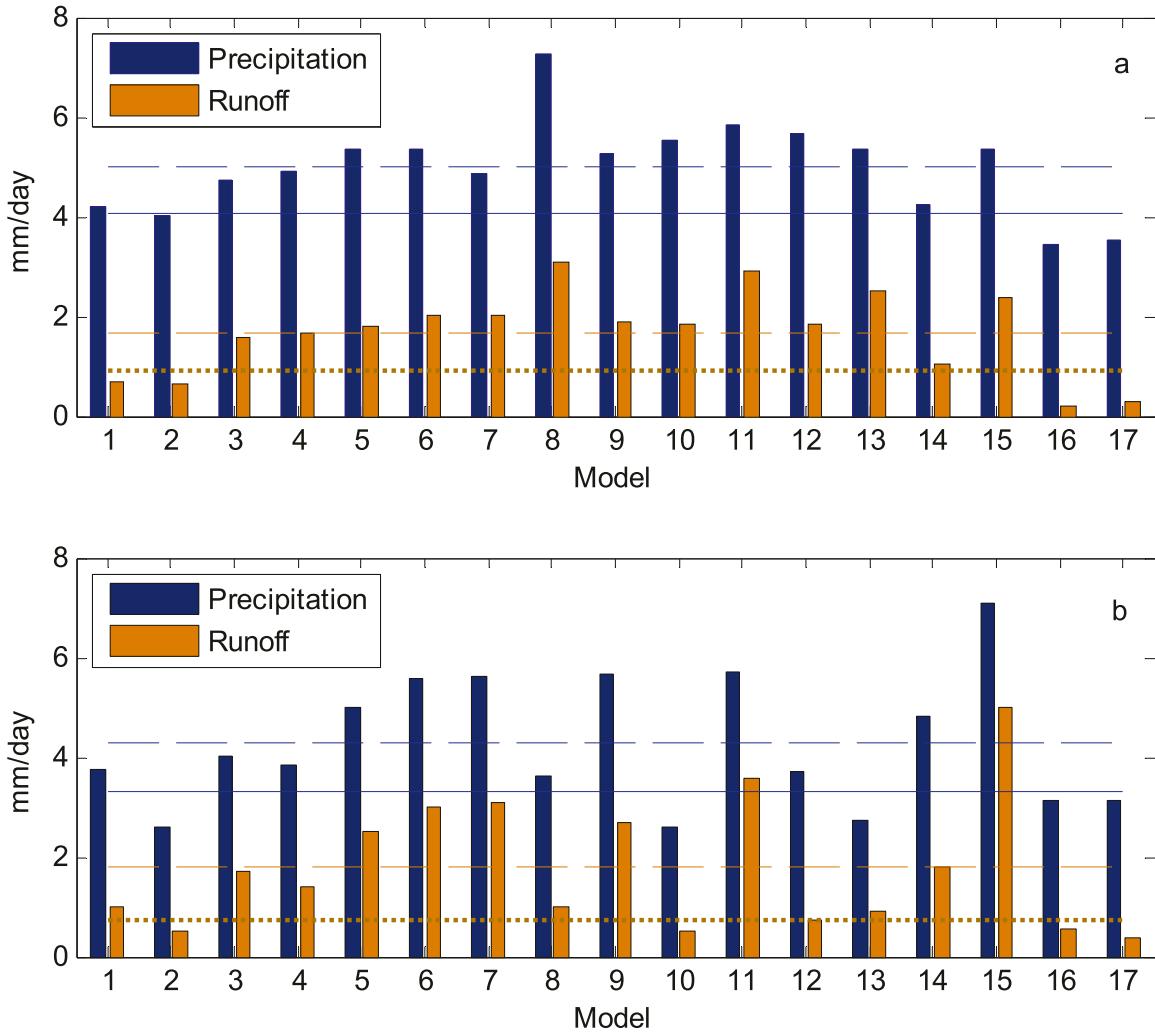
FIG. 4. Analysis of precipitation and runoff of 22 yr (1979–2000) for 17 GCMs of CMIP3 for (a) the Congo and (b) UBN basins. The long-term average of the CRU TS 3.1 precipitation (blue solid line) and the observed streamflow (brown dotted line) are shown. The dashed lines are for the ensemble average. The model number is as listed in Table 3.

a seasonal cycle similar to the observations especially for the Congo basin (Fig. 2f). A detailed analysis of the runoff components (surface and subsurface) can clarify this discrepancy, but the runoff was only available as the sum of surface and subsurface runoff.

A comparison between the spatial distribution of the net precipitation, runoff, and convergence of atmospheric moisture is illustrated in Fig. 3. Their long-term spatial distribution is nearly the same, as expected, except for the convergence of atmospheric moisture near the coastlines. An analysis of the moisture fluxes (not shown here) along the land–ocean boundaries has shown that this significant bias over these regions is induced by the sudden change in magnitude of moisture fluxes between land and ocean. This change is amplified when the derivative of moisture fluxes is calculated. This

can explain the strong convergence and divergence regions that are located beside each other along the Red Sea, Mediterranean Sea, and Persian Gulf area. Another reason for this bias is the strong convergence of moisture fluxes simulated by the ERA-Interim data along the western coast of Africa (Fig. 3).

Although the ERA-Interim product overestimates the hydrological variables compared to observations, it is considered better than the ERA-40 and the NCEP–NCAR products for the studied regions. The ERA-40 and the NCEP–NCAR reanalysis do not satisfy the atmospheric and soil water balances as shown in Table 4, and the simulated seasonal cycle of the hydrological variables did not match the observation as the ERA-Interim (not shown here). This imbalance problem between the long-term averages of the convergence of
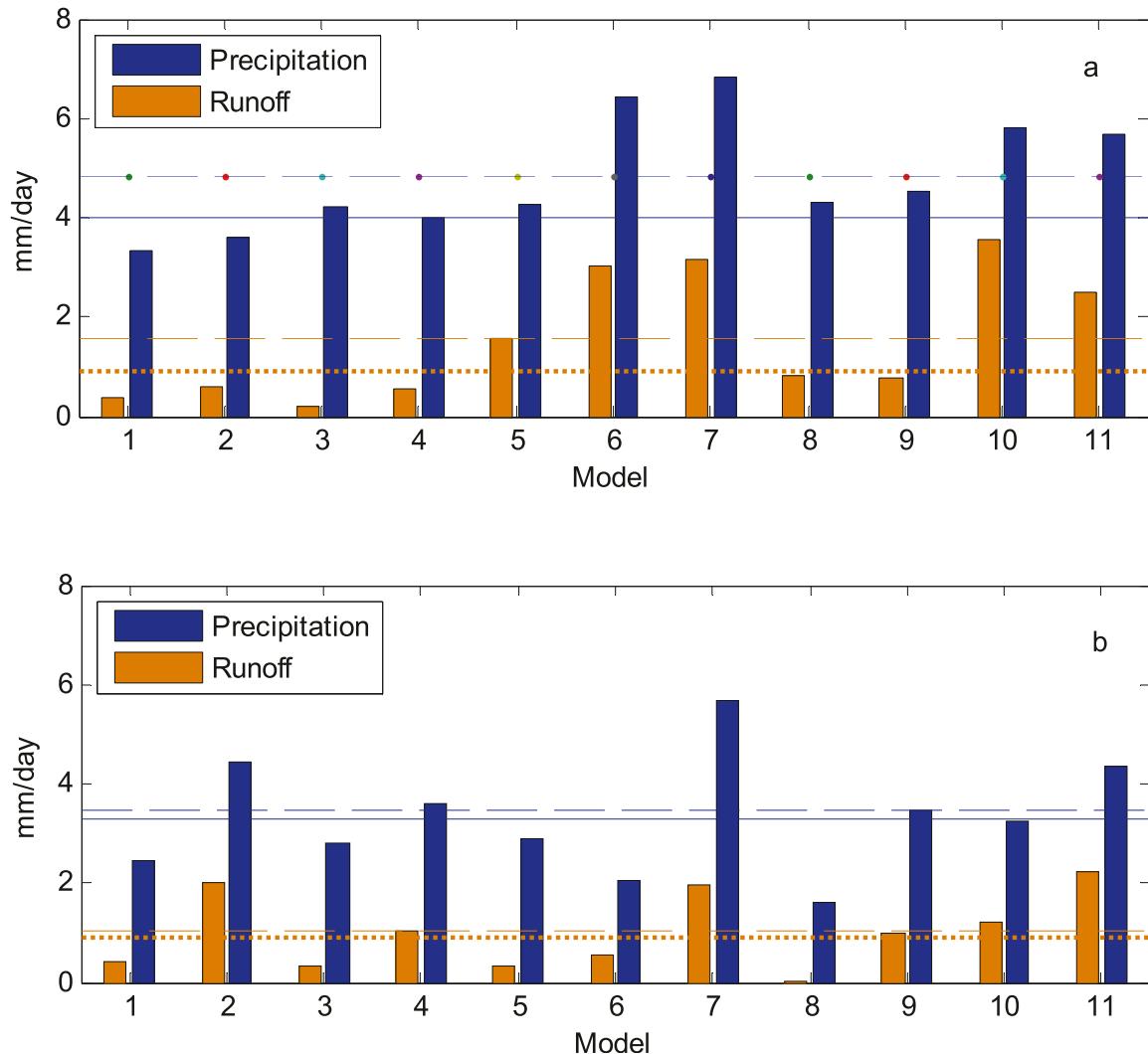
FIG. 5. As in Fig. 4, but for GCMs of CMIP5.

moisture calculated using the reanalysis products and the streamflow was highlighted by Seneviratne et al. (2004) assigning the potential sources of these errors the insufficient spatial and temporal sampling of the radiosondes measurements or errors related to the data assimilation process. For the ERA-40, the water imbalance of the ERA-40 data was noticed by Berrisford et al. (2011) and was adjusted in the ERA-Interim product. However, the results of the ERA-Interim and ERA-40 were better than the NCEP–NCAR for the studied regions. A similar observation was made by Karam and Bras (2008b) for the Amazon basin where they found that the ERA-40 moisture fluxes were more accurate than the NCEP–NCAR, but still both of them are significantly biased. The bias of the NCEP–NCAR fluxes data was shown in similar studies (Ruprecht and Kahl 2003; Maurer et al. 2001; Lenters et al. 2000).

b. The hydrological cycle in CMIP3 and CMIP5 GCMs

In this section, the hydrological cycles of 17 GCMs of the CMIP3 project and 11 GCMs of the CMIP5 project are analyzed. The analysis of convergence of atmospheric moisture is not repeated for these GCMs, as the required outputs for this calculation are not available at suitable time interval (i.e., less than 1 day) for some of the GCMs. However, as land surface schemes and the dynamical cores of these models are coupled without any assimilation of observations, as for the reanalysis products, the potential inconsistency between the atmosphere and land water balance should not exist for these models.

Figures 4 and 5 illustrate the significant biases present in the analyzed GCMs for simulating the precipitation

TABLE 5. Summary of results for CMIP3 GCMs over the Congo and UBN basins.

	Model	Precipitation (mm day^{-1})		Runoff (mm day^{-1})		Evaporation (mm day^{-1})	
		UBN	Congo	UBN	Congo	UBN	Congo
1	HadGEM1	3.77	4.18	1.02	0.70	2.75	3.48
2	MPI ECHAM5	2.58	4.03	0.52	0.63	2.06	3.40
3	CSIRO Mk3.5	4.04	4.73	1.71	1.60	2.33	3.13
4	CSRIO Mk3	3.83	4.91	1.41	1.65	2.42	3.26
5	GFDL CM2.0	5.01	5.34	2.50	1.80	2.51	3.54
6	BCCR-CM2.0	5.59	5.37	3.02	2.03	2.57	3.34
7	MRI-CGCM2.3.2	5.64	4.85	3.11	2.04	2.53	2.81
8	NCAR PCM1	3.63	7.25	1.00	3.10	2.63	4.15
9	CNRM-CM3	5.67	5.25	2.67	1.87	3.00	3.38
10	IAP FGOALS	2.58	5.52	0.52	1.85	2.06	3.67
11	CCCma CGCM(T63)	5.69	5.80	3.56	2.93	2.13	2.87
12	HadCM3	3.69	5.68	0.74	1.83	2.95	3.85
13	IPSL-CM4	2.72	5.37	0.89	2.52	1.83	2.85
14	MIUB-ECHO-G	4.83	4.23	1.78	1.05	3.05	3.18
15	CCCma CGCM(T47)	7.09	5.36	5.00	2.38	2.09	2.98
16	GISS-AOM3.1	3.15	3.45	0.57	0.20	2.58	3.25
17	INM-CM3.0	3.14	3.52	0.38	0.30	2.76	3.22
	Observation	3.3	4.06	0.72	0.9	2.08	2.83

and runoff for the UBN and Congo basins. A general pattern seen in these models is that most of the models, particularly among the CMIP3 models, show a wetter climate by overestimating precipitation and runoff, as reflected by their high model ensemble averages compared to observations (Tables 5 and 6). As the UBN basin is a very small region with complex topography, it is possible that such a bias is the result of the coarse resolution used by some models, rather than due to model formulation. To verify this hypothesis, the CMIP3 and CMIP5 models are sorted in Figs. 4 and 5, respectively, according to their horizontal resolution. In the CMIP3 models, some of the highest- and lowest-resolution models tend to have values of precipitation and runoff close to observations over both the Congo and the UBN basin. These variables are mainly

overestimated for the medium-resolution models. This finding tends to show that the water budget does not depend on model resolution. However, the simulated seasonal cycle of runoff and precipitation in the high-resolution CMIP3 models (Figs. 6a,b) is usually better simulated than in the medium- (Figs. 6c,d) and low- (Figs. 6e,f) resolution models. Similarly, the high-resolution CMIP5 models (Figs. 7a,b) generally show a better simulation of the seasonal cycle compared to the medium-resolution models (Figs. 7c,d).

It can be concluded that the increase in resolution of climate models may improve the representation of the seasonal cycle of hydrological variables. However, increasing horizontal resolution does not remove all the biases in simulating the hydrological cycle and improvements in the simulation of other processes (e.g.,

TABLE 6. Summary of results for CMIP5 GCMs over the Congo and UBN basins.

|	Model	Precipitation (mm day^{-1})		Runoff (mm day^{-1})		Evaporation (mm day^{-1})	
		UBN	Congo	UBN	Congo	UBN	Congo
1	MRI-CGCM3	2.46	3.34	0.40	0.36	2.06	2.97
2	CNRM-CM5	4.44	3.58	2.02	0.59	2.42	2.99
3	INM-CM4.0	2.83	4.23	0.33	0.19	2.50	4.04
4	HadGEM2-CC	3.62	4.10	1.04	0.56	2.58	3.44
5	CSIRO	2.91	4.28	0.33	1.55	2.58	2.73
6	IPSL-CM5-MR	2.06	6.44	0.56	3.02	1.51	3.41
7	NorESM1-M	5.69	6.82	1.95	3.15	3.74	3.66
8	GISS-E2H	1.59	4.30	0.00	0.80	1.59	3.50
9	GFDL CM3	3.45	4.51	1.02	0.78	2.43	3.73
10	BCC-CSM1	3.24	5.90	1.22	3.56	2.02	2.90
11	CanESM2	4.36	5.66	2.25	2.48	2.11	3.18
	Observation	3.3	4.06	0.72	0.9	2.08	2.83
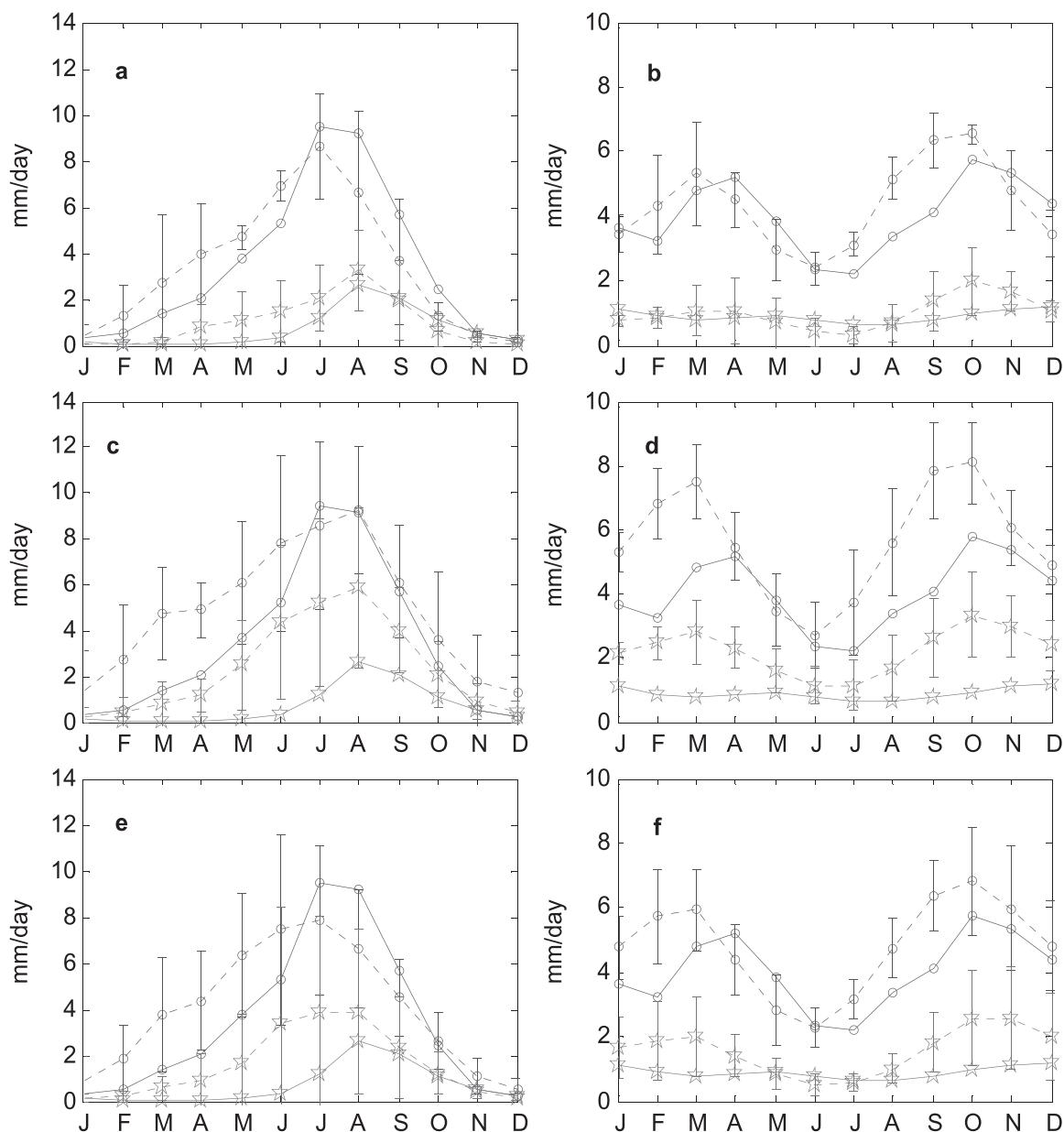
FIG. 6. Seasonal cycle of precipitation and runoff of 22 yr (1979–2000) for 17 GCMs of the CMIP3 for the (left) UBN and (right) the Congo basins. The figures are sorted (top)–(bottom) according to the spatial resolution of the GCMs: (a),(b) the highest-resolution GCMs (models 1–4) of approximately 1.8° × 1.8°; (c),(d) medium-resolution models (models 5–11) of approximately 2.8° × 1.8°; and (e),(f) low-resolution models (models 12–17) of approximately 4° × 3°. The error bars indicate the variation around the ensemble mean of the models of equivalent resolution by one standard deviation. The solid lines with circles and stars are for the long-term averages of observations of precipitation using CRU TS 3.1 and the observed streamflow, respectively; while the dotted lines are for corresponding values from the GCMs.

energy cycle) are required to accurately simulate the hydrological cycle as discussed in the next section. Roeckner et al. (2006) found that the GCMs must have at least medium resolutions to be able to simulate the climate realistically. The transition between resolutions was described by Williamson et al. (1995): they showed that the transition from low to medium resolution is required to capture the climate statistics and the movement

to higher resolution is required to solve the nonlinear processes in the models that forces the medium scale processes in the atmosphere.

5. Conclusions

In this paper, we introduce an evaluation method that analyzes the hydrological cycle represented by GCMs
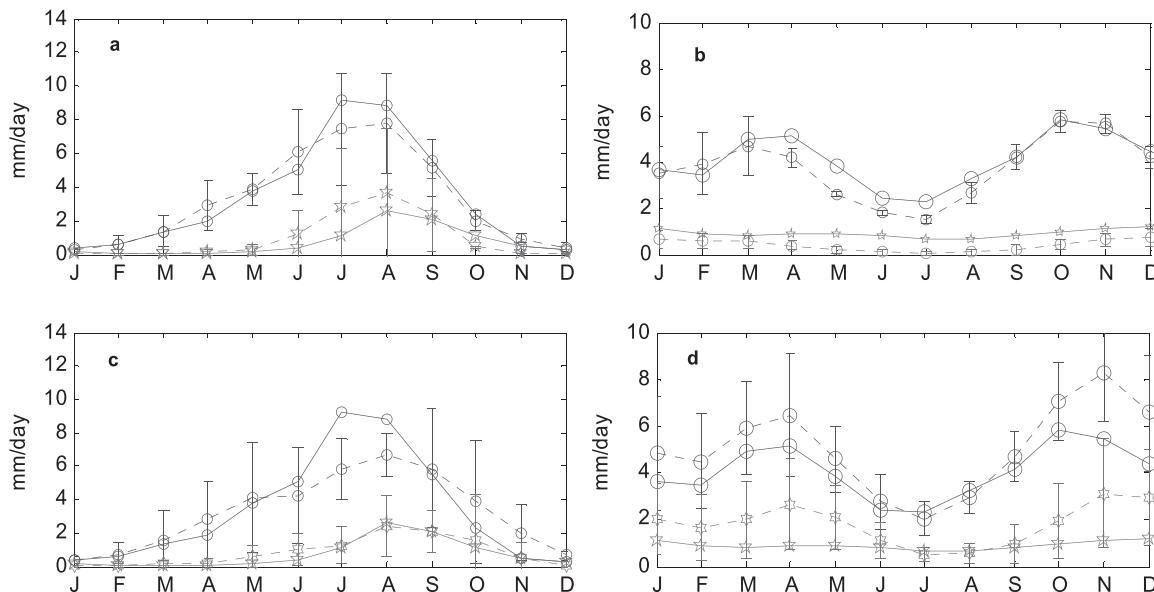
FIG. 7. As in Fig. 6, but for GCMs of CMIP5.

and reanalysis products over the UBN and Congo basins. The method uses the atmospheric and soil water balance approaches to evaluate the ability of GCMs and reanalyses products to reproduce the observed river flow. River flow is one of the best observed and most accurate variable of the hydrological cycle. The use of the observed streamflow as a reference instead of the commonly used variables (e.g., precipitation) therefore allows a reduction in the uncertainties related to observations, which can be of the same order of magnitude as biases in GCMs or reanalyses products.

The evaluation method is first applied for three reanalyses products (ERA-Interim, ERA-40, and NCEP–NCAR). Among them ERA-Interim shows the best performance. It satisfies the atmospheric and soil water balances, represents accurately the seasonal cycle of the hydrological variables and shows a realistic spatial distribution of the moisture fluxes over Africa and the Middle East. This result has important implications for regional climate modeling studies, which often use reanalysis products as boundary conditions and therefore strongly depend on the ability of these products to represent the moisture fluxes at the boundary of the region of study.

Most of the 28 GCMs of the CMIP3 and CMIP5 projects selected for this study simulate a strong bias in the hydrological cycle over the Congo and UBN basins by overestimating precipitation and runoff compared to observations. We studied the relationship between GCM horizontal resolution and their ability to simulate the hydrological cycle over the UBN and Congo basins. It was shown that most of the models with the highest resolution (approximately 200 km) are able to simulate more

accurately the seasonal cycle the hydrological variables compared to the medium- (300 km) and low-resolution (400 km) models over both basins. Several reasons that are under investigation could be responsible for improving the hydrological cycle simulation associated with increasing horizontal resolution. For example, increasing model resolution can enhance the simulation of moisture transport particularly over small-scale basins. In addition, the high-resolution GCMs considered in this study better represent topography, which directly affects the amount and distribution of rainfall, particularly over the UBN basin. The presented analysis gives some guidance for selecting the suitable GCMs to use for climate change studies over the Congo and UBN basins as using only the models that are able to simulate correctly the water cycle can increase the confidence on their future projection of changes in the hydrological cycle.

REFERENCES

Amarasekera, K. N., R. F. Lee, E. R. Williams, and E. A. B. Eltahir, 1997: ENSO and the natural variability in the flow of tropical rivers. *J. Hydrol.,* **200,** 24–39.

Berrisford, P., P. Kållberg, S. Kobayashi, D. Dee, S. Uppala, A. J. Simmons, P. Poli, and H. Sato, 2011: Atmospheric conservation

properties in ERA-Interim. *Quart. J. Roy. Meteor. Soc.,* **137,** 1381–1399.

Boé, J., L. Terray, E. Martin, and F. Habets, 2009: Projected changes in components of the hydrological cycle in French river basins during the 21st century. *Water Resour. Res.,* **45,** W08426, doi:10.1029/2008WR007437.

Calanca, P., and A. Ohmura, 1994, Atmospheric moisture flux convergence and accumulation on the Greenland Ice Sheet. IAHS Publication 223, 8 pp.

Christensen, J. H., and Coauthors, 2007: Regional climate projections. *Climate Change 2007: The Physical Science Basis,* S. Solomon et al., Eds., Cambridge University Press, 847–940.

Conway, D., and M. Hulme, 1993: Recent fluctuations in precipitation and runoff over the Nile subbasins and their impact on main Nile discharge. *Climatic Change,* **25,** 127–151.

——, and ——, 1996: The impacts of climate variability and future climate change in the Nile basin on water resources in Egypt. *Int. J. Water Resour. Dev.,* **12,** 277–296.

Dee, D. P., and Coauthors, 2011: The ERA-Interim reanalysis: Configuration and performance of the data assimilation system. *Quart. J. Roy. Meteor. Soc.,* **137,** 553–597.

Elshamy, M. E., I. A. Seierstad, and A. Sorteberg, 2009: Impacts of climate change on Blue Nile flows using bias-corrected GCM scenarios. *Hydrol. Earth Syst. Sci.,* **13,** 551–565.

Gleckler, P. J., K. E. Taylor, and C. Doutriaux, 2008: Performance metrics for climate models. *J. Geophys. Res.,* **113,** D06104, doi:10.1029/2007JD008972.

Johns, T. C., and Coauthors, 2006: The new Hadley Centre climate model (HadGEM1): Evaluation of coupled simulations. *J. Climate,* **19,** 1327–1353.

Kalnay, E., and Coauthors, 1996: The NCEP/NCAR 40-Year Reanalysis Project. *Bull. Amer. Meteor. Soc.,* **77,** 437–471.

Karam, H. N., and R. L. Bras, 2008a: Climatological basin-scale Amazonian evapotranspiration estimated through a water budget analysis. *J. Hydrometeor.,* **9,** 1048–1060.

——, and ——, 2008b: Estimates of net atmospheric moisture flux convergence over the Amazon basin: A comparison of reanalysis products. *J. Hydrometeor.,* **9,** 1035–1047.

Kim, U., J. J. Kaluarachchi, and V. U. Smakhtin, 2008: Climate change impacts on hydrology and water resources of the upper Blue Nile River basin, Ethiopia. International Water Management Institute Research Rep 126, 27 pp.

Lenters, J. D., M. T. Coe, and J. A. Foley, 2000: Surface water balance of the continental United States, 1963–1995: Regional evaluation of a terrestrial biosphere model and the NCEP/NCAR reanalysis. *J. Geophys. Res.,* **105,** 22 393–22 425.

Maurer, E. P., G. M. O'Donnell, D. P. Lettenmaier, and J. O. Roads, 2001: Evaluation of the land surface water budget in NCEP/NCAR and NCEP/DOE reanalyses using an off-line hydrologic model. *J. Geophys. Res.,* **106,** 17 841–17 862.

Meehl, G. A., C. Covey, K. E. Taylor, T. Delworth, R. J. Stouffer, M. Latif, B. McAvaney, and J. F. B. Mitchell, 2007: The WCRP CMIP3 multimodel dataset: A new era in climate change research. *Bull. Amer. Meteor. Soc.,* **88,** 1383–1394.

Mitchell, T. D., and P. D. Jones, 2005: An improved method of constructing a database of monthly climate observations and associated high-resolution grids. *Int. J. Climatol.,* **25,** 693–712.

Nohara, D., A. Kitoh, M. Hosaka, and T. Oki, 2006: Impact of climate change on river runoff. *J. Hydrometeor.,* **7,** 1076–1089.

Oki, T., K. Musiake, H. Matsuyama, and K. Masuda, 1995: Global atmospheric water balance and runoff from large river basins. *Hydrol. Processes,* **9,** 655–678.

Peixoto, J. P., and A. H. Oort, 1992: *Physics of Climate.* American Institute of Physics, 520 pp.

Perkins, S. E., A. J. Pitman, N. J. Holbrook, and J. McAneney, 2007: Evaluation of the AR4 climate models' simulated daily maximum temperature, minimum temperature, and precipitation over Australia using probability density functions. *J. Climate,* **20,** 4356–4376.

Raisanen, J., 2007: How reliable are climate models? *Tellus,* **59A,** 2–29.

Randall, D. A., and Coauthors, 2007: Climate models and their evaluation. *Climate Change 2007: The Physical Science Basis,* S. Solomon et al., Eds., Cambridge University Press, 589–662.

Rasmusson, E. M., 1967: Atmospheric water vapor transport and the water balance of North America: Part I. Characteristics of the water vapor flux field. *Mon. Wea. Rev.,* **95,** 403–426.

——, 1968: Atmospheric water vapor transport and the water balance of North America. *Mon. Wea. Rev.,* **96,** 720–734.

——, 1971: A study of the hydrology of eastern North America using atmospheric vapor flux data. *Mon. Wea. Rev.,* **99,** 119–135.

Ruprecht, E., and T. Kahl, 2003: Investigation of the atmospheric water budget of the BALTEX area using NCEP/NCAR reanalysis data. *Tellus,* **55A,** 426–437.

Samba, G., and D. Nganga, 2011: Rainfall variability in Congo-Brazzaville: 1932–2007. *Int. J. Climatol.,* **32,** 854–873, doi:10.1002/joc.2311.

Schaller, N., I. Mahlstein, J. Cermak, and R. Knutti, 2011: Analyzing precipitation projections: A comparison of different approaches to climate model evaluation. *J. Geophys. Res.,* **116,** D10118, doi:10.1029/2010JD014963.

Seneviratne, S. I., P. Viterbo, D. Luthi, and C. Schar, 2004: Inferring changes in terrestrial water storage using ERA-40 reanalysis data: The Mississippi River basin. *J. Climate,* **17,** 2039–2057.

Strzepek, K., and D. N. Yates, 1996: Economic and social adaptations to climate change impacts on water resources: A case study of Egypt. *Water Resour. Dev.,* **12,** 229–244.

Taylor, K. E., R. J. Stouffer, and G. A. Meehl, 2012: An overview of CMIP5 and the experiment design. *Bull. Amer. Meteor. Soc.,* **93,** 485–498.

Trenberth, K. E., L. Smith, T. Qian, A. Dai, and J. Fasullo, 2007: Estimates of the global water budget and its annual cycle using observational and model data. *J. Hydrometeor.,* **8,** 758–769.

Uppala, S. M., and Coauthors, 2005: The ERA-40 Re-Analysis. *Quart. J. Roy. Meteor. Soc.,* **131,** 2961–3012.

Vörösmarty, C. J., B. Fekete, and B. A. Tucker, 1998: River discharge database, version 1.1 (RivDIS v1.0 supplement). University of New Hampshire Institute for the Study of Earth, Oceans, and Space.

Williamson, D. L., J. T. Kiehl, and J. J. Hack, 1995: Climate sensitivity of the NCAR Community Climate Model (CCM2) to horizontal resolution. *Climate Dyn.,* **11,** 377–397.

Yates, D. N., and K. M. Strzepek, 1998: An assessment of integrated climate change impacts on the agricultural economy of Egypt. *Climatic Change,* **38,** 261–287.

Yeh, P. J., M. Irizarry, and E. A. B. Eltahir, 1998: Hydroclimatology of Illinois: A comparison of monthly evaporation estimates based on atmospheric water balance and soil water balance. *J. Geophys. Res.,* **103,** 19 823–19 837.

Zhang, K., J. S. Kimball, R. R. Nemani, and S. W. Running, 2010: A continuous satellite-derived global record of land surface evapotranspiration from 1983 to 2006. *Water Resour. Res.,* **46,** W09522, doi:10.1029/2009WR008800.